Atmospheric Environment 182 (2018) 75–86

Contents lists available at ScienceDirect

Atmospheric Environment

journal homepage: www.elsevier.com/locate/atmosenv

Nitrogen deposition in precipitation to a monsoon-affected eutrophic embayment: Fluxes, sources, and processes

Yunchao Wu[a,b], Jingping Zhang[a,**], Songlin Liu[a], Zhijian Jiang[a], Iman Arbi[a,b], Xiaoping Huang[a,b,*], Peter Ian Macreadie[c]

[a] Key Laboratory of Tropical Marine Bio-resources and Ecology, South China Sea Institute of Oceanology, Chinese Academy of Sciences, Guangzhou 510301, China
[b] University of Chinese Academy of Sciences, Beijing 100049, China
[c] Blue Carbon Lab, Centre for Integrative Ecology, School of Life and Environmental Sciences, Faculty of Science Engineering & Built Environment, Burwood, Deakin University, Victoria 3125, Australia

ARTICLE INFO

Keywords:
Nitrogen deposition
Air pollution
Sources
Isotopic composition
Daya bay

ABSTRACT

Daya Bay in the South China Sea (SCS) has experienced rapid nitrogen pollution and intensified eutrophication in the past decade due to economic development. Here, we estimated the deposition fluxes of nitrogenous species, clarified the contribution of nitrogen from precipitation and measured ions and isotopic composition ($\delta^{15}N$ and $\delta^{18}O$) of nitrate in precipitation in one year period to trace its sources and formation processes among different seasons. We found that the deposition fluxes of total dissolved nitrogen (TDN), NO_3^-, NH_4^+, NO_2^-, and dissolved organic nitrogen (DON) to Daya Bay were 132.5, 64.4 17.5, 1.0, 49.6 mmol $m^{-2}{\cdot}yr^{-1}$, respectively. DON was a significant contributor to nitrogen deposition (37% of TDN), and NO_3^- accounted for 78% of the DIN in precipitation. The nitrogen deposition fluxes were higher in spring and summer, and lower in winter. Nitrogen from precipitation contributed nearly 38% of the total input of nitrogen (point sources input and dry and wet deposition) in Daya Bay. The $\delta^{15}N\text{-}NO_3^-$ abundance, ion compositions, and air mass backward trajectories implicated that coal combustion, vehicle exhausts, and dust from mainland China delivered by northeast monsoon were the main sources in winter, while fossil fuel combustion (coal combustion and vehicle exhausts) and dust from PRD and southeast Asia transported by southwest monsoon were the main sources in spring; marine sources, vehicle exhausts and lightning could be the potential sources in summer. $\delta^{18}O$ results showed that OH pathway was dominant in the chemical formation process of nitrate in summer, while N_2O_5 + DMS/HC pathways in winter and spring.

1. Introduction

Emission of reactive nitrogen, including oxidized and reduced inorganic nitrogen and organic nitrogen, to the atmosphere have increased dramatically because of food production and energy consumption (Duce et al., 2008; Galloway et al., 2003, 2008). Globally, nitrogen deposition increased slowly from the 1860s to the 1960s, then rapidly in the past half-century (Galloway et al., 2008). It has been predicted that atmospheric nitrogen deposition to the ocean will reach 77 Tg N·yr^{-1} by 2030, of which more than 45% derives from anthropogenic sources (Altieri et al., 2014; Duce et al., 2008). Such fluxes of anthropogenic nitrogen deposited to the ocean can impact coastal ecosystem functions, especially embayments downwind of densely populated areas (Galloway et al., 2008; Kim et al., 2014). Inputs of biologically available nitrogen from the atmosphere to coastal waters are comparable to that from riverine input (Duce et al., 1991; Spokes and Jickells, 2005). It is estimated that 10% to more than 40% of nitrogen entering estuarine and coastal waters derives from atmospheric sources and has been considered as a major driver of primary production (Owens et al., 1992; Paerl et al., 2002; Valigura et al., 2001). Nitrogen-containing compounds in precipitation provide phytoplankton with nutrients and potentially contribute to eutrophication in estuaries and coastal waters (Galloway et al., 2003).

Identifying the sources of nitrogen in precipitation and their biogeochemical fate is the key managing nitrogen inputs from the atmosphere. Dual isotopes, $\delta^{15}N$ and $\delta^{18}O$, of nitrate have been used to identify the sources and chemical processes of nitrate in the atmosphere (Fang et al., 2011; Hoering, 1957; Michalski et al., 2015). $\delta^{15}N-NO_3$ is

* Corresponding author. Key Laboratory of Tropical Marine Bio-resources and Ecology, South China Sea Institute of Oceanology, Chinese Academy of Sciences, Guangzhou 510301, China.
** Corresponding author.
E-mail addresses: zhangjingping@scsio.ac.cn (J. Zhang), xphuang@scsio.ac.cn (X. Huang).

https://doi.org/10.1016/j.atmosenv.2018.03.037
Received 1 October 2017; Received in revised form 14 March 2018; Accepted 18 March 2018
Available online 20 March 2018
1352-2310/

viewed as a signal for nitrate sources as the N atoms are conservative during the formation of NO_3^- in the atmosphere (Morin et al., 2009; Widory, 2007). $\delta^{15}N-NO_3$ abundance can be used to determine N provenance, for example: +6 to +25.6‰ for coal combustion (Felix et al., 2012; Heaton, 1990), −19.1 to +9.8‰ for vehicle (Walters et al., 2015), −7 to +12‰ for biomass burning (Fibiger and Hastings, 2016), −0.5 to +1.4‰ for lightning (Hoering, 1957), and −50 to −20‰ for biogenic emission (Li and Wang, 2008). $\delta^{18}O\text{-}NO_3^-$ values implicate the oxidation pathway involved with oxidants as O_3, free radical like hydroxy (OH), peroxy and halogen. There are two main pathways, (1) OH radical pathway (+55‰), 2/3 O_3 and 1/3 OH radical; (2) N_2O_5 pathway (+102‰), 5/6 O_3 and 1/6 H_2O, for the formation of oxygen atoms in nitrate (Fang et al., 2011; Hastings et al., 2003). 76% and 18% of annual inorganic NO_3^- are formed via the OH pathway and the N_2O_5 pathway, respectively. Moreover, dimethylsulfide (DMS) and hydrocarbons (HC) (DMS/HC) pathway is another important pathway in forming oxygen atoms of nitrate in recent years, which accounts for 4% of the annual inorganic NO_3^- (Alexander et al., 2009; Fang et al., 2011). NO_3^- induced via the DMS/HC pathway have higher $\delta^{18}O$ values than those via the OH pathway and the N_2O_5 pathway due to the involvement of O_3 (Hastings et al., 2003).

China's coastal areas are hotspots of nitrogen emissions and deposition (Liu et al., 2011). A recent study reported that nitrogen deposition averaged 282 mmol·$(m^2 \cdot yr)^{-1}$ within China's coast during 2010–2012, of which wet deposition account for 54.6% (Luo et al., 2014). Daya Bay, located on the north coast of the South China Sea (SCS), is surrounded by densely populated land with rapid industrial growth along the Pearl River Delta (PRD), an economic hub in south China. Industrial development has increased considerably during the past 30 years along Daya Bay's coast, including the petrochemical industry, nuclear and coal-fired power plants, and marine aquaculture. The drastically increasing input of nutrients has induced eutrophication in Daya Bay (Yu et al., 2007). To our knowledge, the deposition flux of nitrogen in precipitation in rainy seasons (March to August in 2012) (Chen et al., 2014) and incomplete annual data (a field observation from August 2008 to July 2009, but no data from November 2008 to February 2009) (Zou et al., 2011) were reported. Daya Bay is a semi-enclosed bay with relative lower water exchange ability. And the nitrogen emission continues to increase in this region. On the basis of understanding the dry deposition flux (Wu et al., 2018) and riverine input (Ren et al., 2013) of nutrients in Daya Bay, therefore, it is urgent to provide annual data of wet deposition fluxes of nitrogenous species for systematic calculation the budget of nitrogen deposition and quantifying its ecological effects on Daya Bay. Moreover, Daya Bay is under the influence of the East Asian monsoon system, whereby strong northeast winds prevail in winter and southwest winds in spring. However, the sources of nitrogen deposited from the atmosphere to the Daya Bay under the co-effect of air pollution and monsoon climate are unknown. This research, which was conducted over one-year of field sampling, aims to provide a preliminary understanding of the input flux and sources of nitrogen in precipitation in Daya Bay under the combined effects of monsoon and anthropogenic pollution.

In this study, concentrations and fluxes of nitrogenous species, ion composition and dual isotopes ($\delta^{15}N\text{-}NO_3^-$, and $\delta^{18}O\text{-}NO_3^-$) of nitrate in precipitation in Daya Bay were measured to identify nitrogen inputs, estimate the sources of the main nitrogen inputs and discuss the depositional processes among different seasons.

2. Materials and methods

2.1. Sampling description

Daya Bay is a semi-enclosed subtropical embayment located in 22.45–22.83°N, 114.50–114.89°E on the northern coast of SCS (Fig. 1). It is one of the largest bays of south China, with an area of ~600 km^2. The average annual temperature (22 °C) and precipitation (1948 mm) are controlled by subtropical and monsoonal climate of East Asia. 14 typhoons traverse the SCS in summer and autumn annually (Huang and Guan, 2012), half of which invade or influence Daya Bay on average. March to August is considered as rainy months, with > 70% of precipitation occurring during this period, whereas September to February is considered as the dry months. In this study, we defined September to November as autumn, December to February as winter, March to May and June to August as spring and summer, respectively. There are 12 rivers around Daya Bay, of which Dan'ao river is the largest (Fig. 1). There are petrochemical bases in the north and aquaculture areas in the northeast and southwest. Two nuclear power stations (NPS) and the Pinghai coal-fired power plant in Daya Bay are operating in this area. Since the 1980s, there have been a rapid expansion of aquaculture, industrial and agricultural activities in the area, with simultaneous developments in tourism and the construction of harbours and highways.

Sampling was done at the Daya Bay Marine Biology and Resources Station (MBRS), located within a distance of 50 m to the coastline, during October 2015 to September 2016. Deposition flux samples were collected using an automatic ZJD-II wet deposition sampler (Zhejiang Hengda™, China). The sampler has been successfully deployed to collect wet deposition of nutrients and trace elements in previous studies (Huang et al., 2010; Xing et al., 2017). The sampler would immediately open its lid when it detected the rain, close the lid and seal the cylinder automatically once the rainy event ended. The sampling cylinder was positioned 1 m above the ground to prevent dust from dropping in. Rainwater samples were collected every rainy day (except some rainfalls < 1 mm). A total of 125 precipitation samples were obtained during this one year sampling period. The precipitation was filtered through a glass fibre membrane (Whatman) using pre-cleaned plastic filtration unit (Nalgene Filterware) and stored in wide-mouth polypropylene (PP) bottles under −20 °C. Precipitation samples were mixed every individual month for the measurements and calculation of VMW concentration and monthly deposition flux. Additional rainwater samples (n = 34) for ions and dual isotope of nitrate ($\delta^{15}N\text{-}NO_3$ and $\delta^{18}O\text{-}NO_3$) were also collected in the rainy event (rainfall ≥ 10 mm) in the middle week of every month during the one-year sampling period. Field blanks were also collected simultaneously in another pre-cleaned cylinder by rinsing with ultra-purewater when the rain event stopped at the sampling site, but the sampling duration period was only 5 min. All the filtrated rainwater was stored in brown PP bottles at −20 °C until analysis.

2.2. Air mass backward trajectory

Air mass backward trajectory analysis was performed to recognized the transport routes using the Hybrid-Single Particle Integrated Trajectory Model (HYSPLIT 4), provided by the Air Resource Laboratory of U.S. National Oceanic and Atmospheric Administration (NOAA) (Rolph et al., 2017; Stein et al., 2015). The backward air mass trajectory was generated for 24 h back in time with 500 m-agl ending level. The backward air mass trajectories were performed and clustered to show the routes of air masses passing through Daya Bay based on the meteorological data from NCEP's Global Data Assimilation System (GDAS, global, 09/2007–present).

2.3. Chemical and isotopic analyses

Total dissolved nitrogen (TDN) was measured using a TOC-L automatic analyzer (Shimadzu™, Japan). NH_4^+ was measured by hypobromite oxidation method, NO_3^- with zinc-cadmium reduction method, and NO_2^- with N-(1-naphthyl) ethylenediamine hydrochloride spectrophotometric method. Dissolved organic nitrogen (DON) was determined by subtracting dissolved inorganic nitrogen (DIN) from the TDN (DON = TDN − DIN). The precisions and recoveries for all

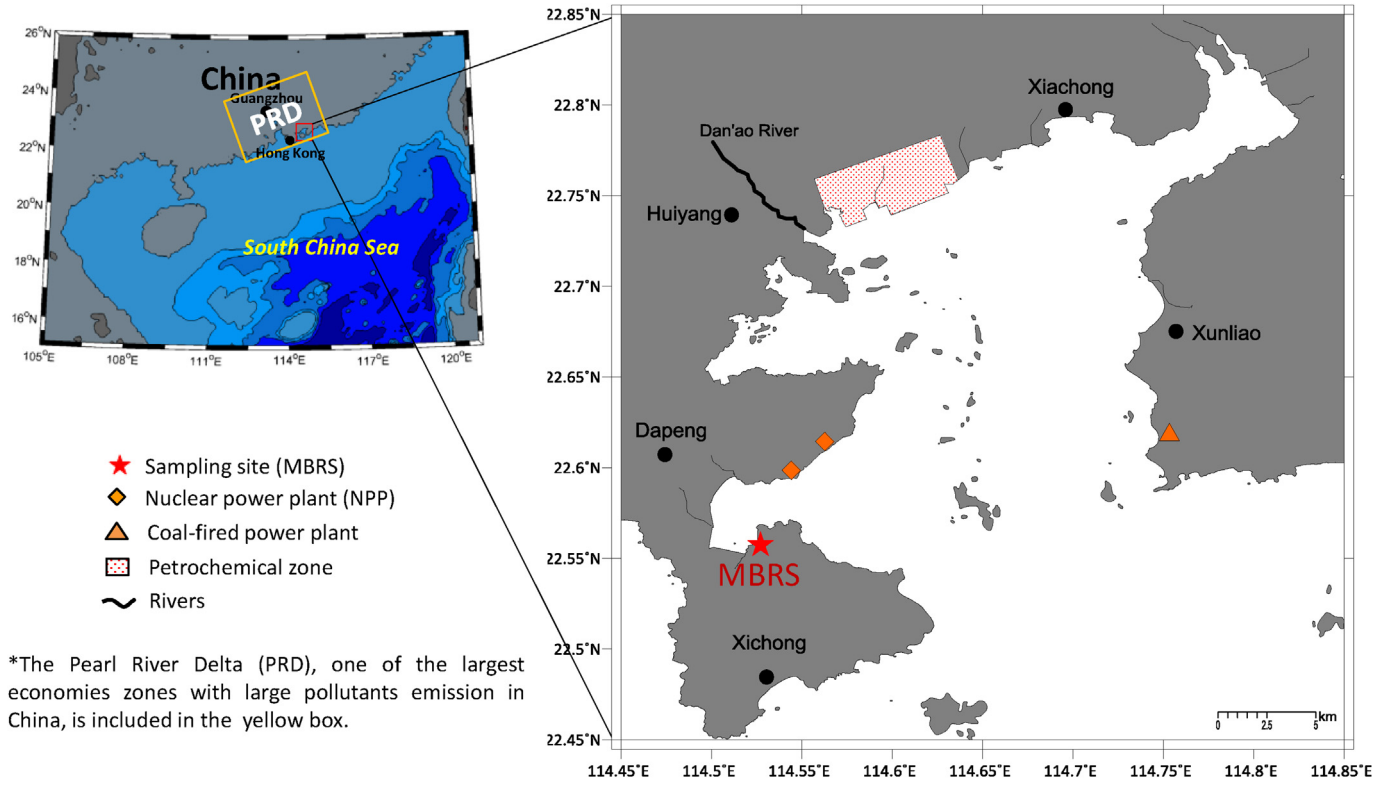

Fig. 1. Sampling site in Daya Bay (MBRS).

nutrient species were better than 5% and between 96.0 and 103.2%, respectively.

Major ionic species (Cl^-, SO_4^{2-}, NO_3^-, Na^+, Mg^{2+}, K^+, Ca^{2+}, NH_4^+) of the additional rainwater samples were individually analyzed by ion chromatography using an ion chromatograph (Dionex, model ICS-2 500), in units of $mg{\cdot}L^{-1}$ and then transformed to $meq{\cdot}L^{-1}$. The concentration of non-sea-salt SO_4^{2-} ($_{nss}SO_4^{2-}$) was calculated by subtracting sea-salt SO_4^{2-} ($_{ss}SO_4^{2-}$), which was estimated by multiplying Na^+ by a factor of 0.252, from total SO_4^{2-} (Yang et al., 2014). Similar methods were used to calculate non-sea-salt K^+ ($_{nss}K^+$) and non-sea-salt Ca^{2+} ($_{nss}Ca^{2+}$) with a coefficient of 0.038 and 0.022, respectively. Nitrogen and ions concentration of blank samples was shown in Table 1. All observed results were blankly corrected.

Dual isotopes ($\delta^{15}N\text{-}NO_3$ and $\delta^{18}O\text{-}NO_3$) of nitrate (34 samples) were measured by denitrifier method (Sigman et al., 2001). A batch of denitrifier strain, *Pseudomonas aureofaciens*, was cultured to denitrify nitrate to N_2O (NO_2^- was insignificant lower (less than 1%) in comparison to NO_3^-, it is not considered here). Subsequently, the dual isotopes of N_2O gas were determined online using a GasBench II coupled with a continuous flow isotope ratio mass spectrometer (IRMS, Thermo Finnigan DELTA^{plus}). The $\delta^{15}N\text{-}NO_3$ were calibrated with USGS32 (180.0 ± 1.0‰ for $\delta^{15}N$), USGS34 (−1.8 ± 0.2‰ for $\delta^{15}N$) and IAEA N3 (4.7 ± 0.2‰ for $\delta^{15}N$), $\delta^{18}O\text{-}NO_3^-$ were calibrated with USGS34 (27.8 ± 0.4‰ for $\delta^{18}O$), IAEA N3 (25.6 ± 0.4‰ for $\delta^{18}O$) and USGS35 (56.8 ± 0.3‰ for $\delta^{18}O$). The accuracy of isotopic analysis is better than ± 0.2 and ± 0.5‰ for $\delta^{15}N\text{-}NO_3$ and $\delta^{18}O\text{-}NO_3$, respectively.

Table 1
Nitrogen and ions species concentration of blank samples (n = 12).

Nitrogen and ion species	Concentration ($\mu mol{\cdot}L^{-1}$)
TDN	0.30 ± 0.12
Na^+	0.42 ± 0.31
Mg^{2+}	0.62 ± 0.20
K^+	0.43 ± 0.20
Ca^{2+}	0.69 ± 0.25
NH_4^+	0.19 ± 0.03
Cl^-	0.65 ± 0.35
SO_4^{2-}	0.49 ± 0.37
NO_3^-	0.20 ± 0.21
NO_2^-	0.02 ± 0.03
DON	0.12 ± 0.07

2.4. Deposition flux estimation and isotope calculation

The volume-weighted mean (VWM) concentrations of nitrogenous species were calculated using Eq. (1) and deposition fluxes of nitrogen were estimated by Eq. (2) as reported by Duce et al. (1991) using the following formulas:

$$C_{VWM} = \Sigma(C_n \times H_n)/\Sigma H_n \quad (1)$$

$$F_w = 0.001 \times \Sigma(C_n \times H_n) \quad (2)$$

where C_{VWM} ($\mu mol{\cdot}L^{-1}$) is the VWM concentration of nitrogenous species; F_w ($mmol{\cdot}m^{-2}$) is the deposition flux of nitrogen; C_n ($\mu mol{\cdot}L^{-1}$) is the concentration of nitrogenous species; H_n (mm) is rainfall amount in every rain event, and n refers to the precipitation event in a certain period.

The dual isotopic compositions of NO_3 ($\delta^{15}N\text{-}NO_3$ and $\delta^{18}O\text{-}NO_3$) were reported as the δ notation according to Eq. (3)

$$\delta\ (‰) = ((R_{Sample}/R_{Standard})\text{-}1) \times 1\,000 \quad (3)$$

where R denotes the ratios of the heavy isotope to light isotope for N and O, in units of per mil (‰).

2.5. Data analysis

All data in different seasons were first tested to determine if the assumptions of homogeneity and normality were met. Differences in $\delta^{15}N\text{-}NO_3^-$ and $\delta^{18}O\text{-}NO_3^-$ between different seasons were assessed with

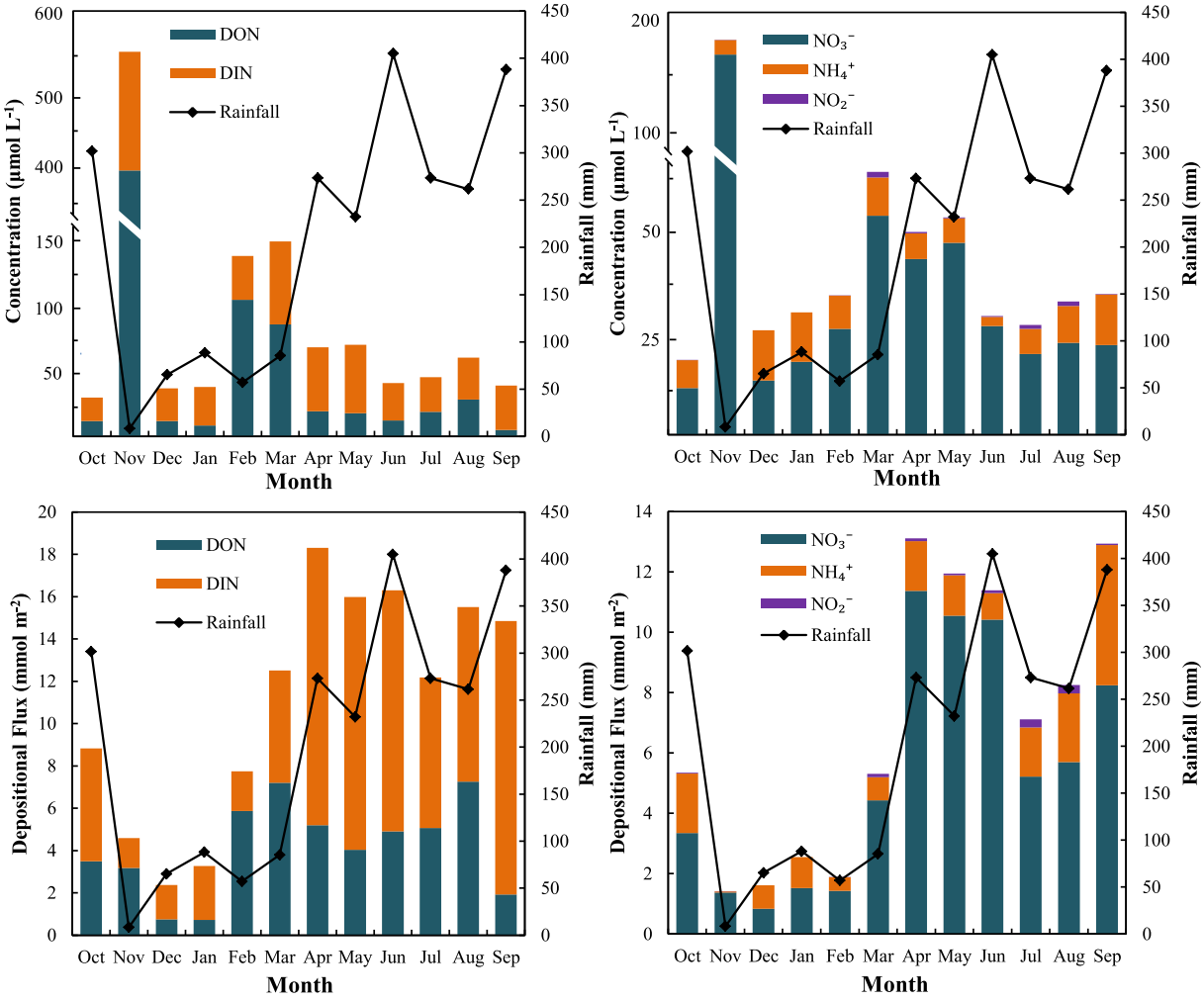

Fig. 2. Time series of concentration and deposition fluxes of nitrogenous species in precipitation and rainfall from October 2015 to September 2016.

independent sample *t*-tests. Regression analyses were used to examine the relationships among different parameters. Significance levels are reported as significant if $p < 0.05$. Statistical analyses including mean values and differences were performed with IBM SPSS 19.0 software.

3. Results and discussion

3.1. Concentration of nitrogen in precipitation

The time series data of the nitrogen concentration and atmospheric nitrogen deposition flux in precipitation and rainfall for each month are illustrated in Fig. 2. The concentration of TDN varied from 29.3 to 556.5 μmol L^{-1}, with an annual VWM concentration of 54.3 μmol L^{-1}. TDN concentration present contrary variation trend and negatively correlated with rainfall ($r = 0.58$, $p < 0.05$). This is partially due to the strong dilution effects of the higher rainfall in rainy seasons (Laouali et al., 2012). VMW concentration of DIN (60% of the TDN) was higher than DON, and NO_3^- was the predominant species of DIN (75% on average). Concentration of nitrogen in precipitation in Daya Bay was remarkably lower than that in northern China coast (VMW concentration was 223.3 μmol L^{-1} Jiaozhou Bay) (Xing et al., 2017) and most of the mainland cities in China (Liu et al., 2013), probably due to the higher annual rainfall and lower nitrogen emission in Daya Bay.

Distinct monthly variation was also observed among the nitrogenous species. The highest concentration of nitrogen was in November, which was also with the lowest rainfall (8 mm). This scale of nitrogen was 3–10 times higher compared with other months and may be due to the longer residence time of ambient aerosols in this month (Liu et al., 2017; Zhang et al., 2001). Except for November, the nitrogen concentration in spring (March to May) was relatively higher, especially for DON, which was also found in north China plain (Zhang et al., 2012). VWM concentration of NO_3^-, which had the highest concentration in spring as well, accounted for 78% of DIN. It should be noted that these maximum concentrations of the nitrogenous species occurred in a season with relatively more rainfall in the wet season. In addition, aerosols in spring mostly originated from the PRD (see discussion below) where there were more industrial activities and anthropogenic emissions, which could be the main reason ascribe to the higher concentration in spring.

3.2. Deposition fluxes of nitrogenous species

Atmospheric nitrogen deposition flux in precipitation and rainfall for each month are illustrated in Fig. 2. TDN deposition flux varied from 2.4 to 18.3 mmol m^{-2}·$month^{-1}$. DIN flux varied from 1.4 to 13.1 mmol m^{-2}·$month^{-1}$, while DON flux varied from 0.7 to 7.3 mmol m^{-2}·$month^{-1}$. DIN and DON made up 62.6% and 37.4% of TDN, respectively (Fig. 3). Deposition flux of TDN in precipitation in this study (11.1 mmol m^{-2}·$month^{-1}$) to Daya Bay was 2.5 times higher compared with that in 2008 (4.5 mmol m^{-2}·$month^{-1}$) (Zou et al., 2011) (Table 2). Another study conducted in rainy months from March to August in 2012 showed that the average monthly deposition flux in precipitation was 14.8 mmol m^{-2}·$month^{-1}$ (Chen et al., 2014). Nitrogen deposition in Daya Bay was at a moderate level compared with

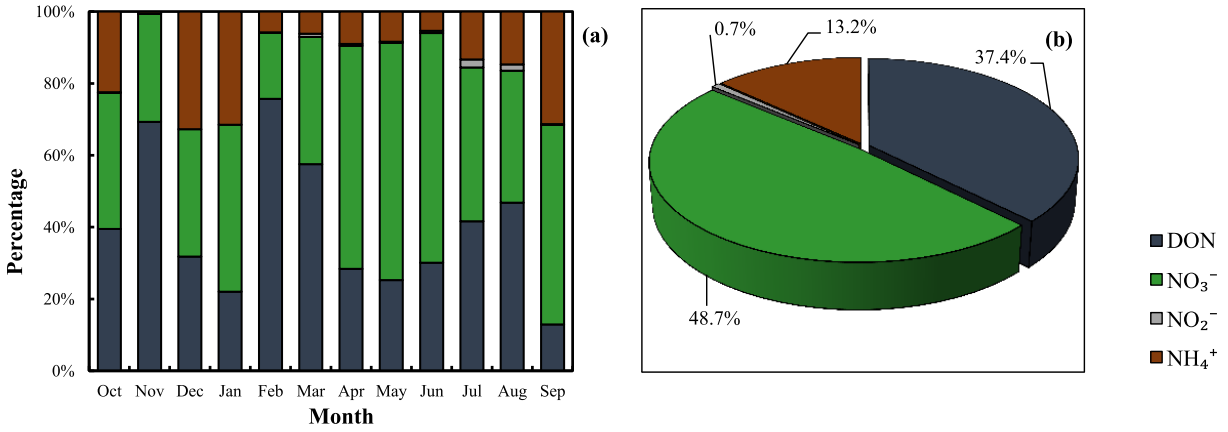

Fig. 3. Composition ratio of nitrogen: (a) monthly and (b) 1-year in total.

other coastal sites in China, but higher than most of the coastal sites worldwide (Gioda et al., 2011; Violaki et al., 2010; Zamora et al., 2011) except Singapore (Table 2) (Karthikeyan et al., 2009). However, it was lower than PRD (Table 2) (Chen et al., 2010), which is one of the most developed regions with the largest nitrogen emission hotspots in China (Huang et al., 2015; Liu et al., 2013).

For the composition of DIN, NO_3^- flux ranged from 0.8 to 11.4 mmol m^{-2}·$month^{-1}$ with an average value at 5.4 ± 3.9 mmol m^{-2}·$month^{-1}$, while NH_4^+ from 0.03 to 4.6 mmol m^{-2}·$month^{-1}$ with an average value at 1.5 ± 1.2 mmol m^{-2}·$month^{-1}$. Nitrate and ammonium accounted for more than 99% of DIN. NH_4^+/NO_3^- ratios in precipitation over the entire sampling period varied from 0.02 to 0.92, with lower ratios in the rainy months (range 0.08–0.40; average 0.21), and higher ratios in the dry months (range 0.02–0.92; average 0.51). The overall mean NH_4^+/NO_3^- ratio (0.36) indicated the dominance of nitrate in atmospheric inorganic nitrogen in precipitation. This was similar to previous studies in Guangzhou and Dongsha Island (north SCS) (Jia and Chen, 2010; Yang et al., 2014), and is consistent with the conclusion that NH_4^+/NO_3^- ratios in coastal area are opposite to Chinese inland cities (Xu et al., 2015), where ammonium is the dominant inorganic nitrogen species (Xing et al., 2017; Zheng et al., 2014). In fact, NH_4^+/NO_3^- ratio is experiencing a decreasing trend from 5 to 2 in China in the past decade due to the increase of nitrogen oxidants (Liu et al., 2013). Moreover, the decrease of the NH_4^+/NO_3^- ratio (0.81 in 2008 (Zou et al., 2011),) implied that the emission of NO_x is rapidly increasing. The low ratio of NH_4^+/NO_3^- agreed well with the decrease in the ratio of calculated emissions of NH_3 to NO_x (Liu et al., 2017), reflecting a more rapid increase in NO_x emissions from industrial and traffic sources. A significantly lower NH_4^+/NO_3^- ratio was found in Daya Bay compared with nitrate dominant coastal cities of China, like Qingdao, Fenghua, Fuzhou, etc. (Luo et al., 2014).

According to the previous studies, the ratio of DON/TDN varied substantially worldwide, between 11 and 42% (Chen et al., 2015; Cornell, 2011; Gioda et al., 2011; Keene et al., 2002). In this study, DON accounted for 37.4% of TDN. Especially in dry months, DON accounted more than 50% of TDN (February and March). As has been found in previous studies in the inland cities in China (Liu et al., 2016), DON deposition had higher deposition flux and contribution to TDN in

Table 2
Nitrogen deposition in precipitation at different coastal areas (all the data in this table are unified with unit mmol m^{-2} mon^{-1}).

Sampling	Date	Rainfall (mm)	Fluxes (mmol m^{-2} mon^{-1})[a]					Ref.
			TDN	DON	NO_3-N	NH_4-N	NO_2-N	
Northern South China Sea								
Pearl River Delta	2006.9–2007.12	–	13.2	4.8	3.4	5.0	–	(Chen et al., 2010)
Zhanjiang	2010.8–2012.5	1952	–	–	7.1	7.9		(Luo et al., 2014)
Daya Bay	2008.8–2009.7[b]	–	4.5	0.2	2.4	1.9	–	(Zou et al., 2011)
	2015.10–2016.9	2 438	11.1	4.1	5.4	1.4	0.2	This study
Other Coastal Sites in China								
Xiamen, Fujian	2004–2005	1 023	15.0	–	–	–		(Chen et al., 2011)
Dalian, Liaoning	2010.9–2012.4	660	–	–	5.4	4.8	–	(Luo et al., 2014)
Changdao, Shandong	2010.9–2012.6	531	–	–	5.3	4.2	–	
Linshan, Shandong	2011.2–2012.5	731	–	–	5.0	4.4	–	
Fenghua, Zhejiang	2010.8–2012.5	1 120	–	–	6.9	5.9	–	
Fuzhou, Fujian	2010.4–2012.6	1 528	–	–	4.2	4.3	–	
Jiaozhou Bay (QD)	2015.6–2016.5	860	16.3	3.8	4.5	7.6	0.4	(Xing et al., 2017)
Other Worldwide Sites								
Charlottesville (USA)	1997.5–1997.8	1 390	5.6	0.5	2.8	2.3		(Keene et al., 2002)
Sandy hook (USA)	1998–1999	–	–	–	3.8	2.0	–	(Gao et al., 2007)
Tuckerton (USA)	1999–2001	–	–	–	2.4	1.6	–	
Tampa Bay, FL (USA)	2005.7–2005.9	1 330	6.4	0.5	4.5	1.4		(Calderon et al., 2007)
Miami (USA)	2008–2009	1 490	2.3	0.02	1.2	0.9		(Zamora et al., 2011)
Luquillo (Puerto Rico)	2004.12–2007.3	1 041	1.4	0.6	0.5	0.3		(Gioda et al., 2011)
Singapore	2007.3–2007.4	1730	33.7	12.3	19.4	2.0		(Karthikeyan et al., 2009)
Eastern Mediterranean (Greece)	2003–2006	550	1.8	0.4	0.8	0.6		(Violaki et al., 2010)
North Sea (Belgium)	2004–2006	420	2.9	0.1	1.2	1.6		(Bencs et al., 2009)

- in the table implies no exact data.
[a] Fluxes are based on the existing valid data.
[b] No data from Nov. 2008 to Feb. 2009.

Table 3
Seasonal and annual deposition flux (mmol·m^{-2}) and VWM concentration (μmol·L^{-1}) of nitrogen at Daya Bay.

Year	Sampling period	Deposition fluxes/VWM concentration					Rainfall (mm)
		TDN	DIN			DON	
			NO_3^-	NH_4^+	NO_2^-		
2015–2016	Autumn	28.2/40.5	13.0/18.6	6.7/9.5	0.06/0.09	8.6/12.3	698
	Winter	13.4/63.6	3.8/18.2	2.3/10.7	0.01/0.01	7.4/34.9	210
	Spring	46.8/79.3	26.3/44.6	3.7/6.4	0.27/0.45	16.4/27.8	591
	Summer	44.0/46.8	21.3/22.7	4.8/5.1	0.63/0.68	17.3/18.3	939
	1-year average	11.0/54.3	5.4/26.4	1.5/7.2	0.08/0.39	4.1/20.3	2 438

spring (Zhang et al., 2012), which is in accordance with the variation of the DON concentration in Daya Bay. Based on this point, we may conclude that DON plays a ubiquitous role and is a significant contributor to nitrogen deposition in precipitation in Daya Bay. Given the importance of DON, we recommend further studies on the $\delta^{15}N$ isotope signature of DON to identify the specific sources.

3.3. Seasonal patterns

Seasonal patterns, with high fluxes of nitrogenous species (except NH_4^+) in rainy months (spring and summer) and low fluxes in dry months (autumn and winter), of nitrogen deposition fluxes were presented in Table 3. DIN accounted for the predominant part of TDN in precipitation, which is contrary to that DON was the main part in the dry deposition (Wu et al., 2018). DIN fluxes (including NO_3^- and NH_4^+) were well correlated with rainfall, while DON showed no strong correlation with rainfall (Table 4). Moreover, higher DIN/TDN ratio was also found in spring. This may suggest that inorganic nitrogen in the aerosol was strongly scavenged by rainfall. Similar results were observed in the coast of Yellow Sea of China (Qi et al., 2013; Xing et al., 2017) and the southern East China Sea (Chen et al., 2015), indicating that rainfall is an important factor controlling the deposition flux of inorganic nitrogenous species (Fig. 2, Table 4). Nitrogen deposition flux and VWM concentrations of TDN and nitrate were higher in spring (Table 3). On the contrary, the maximum ammonium deposition flux and VWM concentration occurred in autumn, which differs with other nitrogenous species. The similar seasonal pattern of ammonium was found in the Yangtze River Delta (Meng et al., 2014), another major economic zone in eastern China coast. This coincided with the active agricultural activities from mainland China (Chen et al., 2011), which may cause the higher ammonium deposition flux in autumn. However, both higher concentration and contribution of DON were found in winter (Table 3). The organic fraction depends on the seasonal biological emissions and long-range transport (Gioda et al., 2011), which could be ascribed to the anthropogenic activities and the northeast monsoon from the continental sources (Zhang et al., 2012). And this pattern was also found in Fuzhou (Zhang et al., 2012) and Jiaozhou Bay (Xing et al., 2017).

Table 4
Correlation matrix of nitrogen species fluxes in precipitation at Daya Bay (performed with the mean value in 12 months).

	Rainfall	TDN	DIN	DON	NO_3^-	NO_2^-	NH_4^+
Rainfall	1.00	0.75**	0.84**	0.13	0.76**	0.39	0.69*
TDN		1.00	0.92**	0.59*	0.92**	0.55	0.46
DIN			1.00	0.23	0.97**	0.35	0.62*
DON				1.00	0.29	0.64*	0.13
NO_3^-					1.00	0.32	0.41
NO_2^-						1.00	0.22
NH_4^+							1.00

*$p < 0.05$.
**$p < 0.01$.

Table 5
Nutrient input from wet deposition, dry deposition and riverine in Daya Bay.

	TDN (t/a)	NO_3^- (t/a)	NH_4^+ (t/a)	NO_2^- (t/a)	DON (t/a)
Wet deposition	1 118.8	544.3	141.1	20.1	413.3
Dry deposition[a]	216.4	71.0	7.8	0.5	137.1
Riverine input[b]	1 626.7	278.7	1 018.0	168.2	161.8
Wet deposition ratio	37.8%	60.9%	12.1%	10.6%	58.0%

[a] Dry deposition data was from Wu et al. (2018).
[b] Riverine input data was from Ren et al. (2013).

3.4. Contribution and effect of nitrogen in precipitation in Daya Bay

The deposition flux of TDN in precipitation could reach to 1 118.8 t/a (in ~600 km^2) during our sampling period (Table 5). We combined point sources discharge (including riverine input and waster water drainage) and atmospheric input (dry and wet deposition) as the total input of nitrogen. Nitrogen in precipitation was the predominant contributor from the atmosphere (84%, nitrogen from dry deposition was 216.4 t/a, see Wu et al. (2018)). This scale of TDN from wet deposition could account for 37.8% of the total nutrient input in Daya Bay. Especially, NO_3^- and DON accounted for nearly 60% of all the nitrogen input. Atmospheric deposition of nitrogen plays a more important role in Daya Bay. It is widely accepted that riverine inputs are the dominant contributor of nitrogen in coastal waters. However, riverine input was relatively lower in Daya Bay compared with other embayments (Kocak et al., 2010; Xing et al., 2017) because of the fewer rivers discharge. Moreover, nitrogen concentration in precipitation was obviously higher than that in the seawater (Wang et al., 2008; Wu et al., 2017), which may enrich the seawater and lead to the rapid growth of phytoplankton in a short period (Paerl et al., 2002; Xu et al., 2014). Considering the deposition flux of nitrogen and DIN/DIP ratio (407:1 on a molar basis, unpublished data), nitrogen input from precipitation throughout the year may cause ecological effects on the embayment ecosystem, such as eutrophication or deterioration of the unbalanced nutrient structure (Wu et al., 2017; Xu et al., 2014).

3.5. Potential sources of nitrate in precipitation

In this study, 34 heavy precipitation samples were collected and they were suitable to represent the source contributions over the entire

Table 6
Ranges of seasonal isotopes values in precipitation in Daya Bay.

Stage	(δ^{15}N-NO_3^-) (‰)		(δ^{18}O-NO_3^-) (‰)	
	Mean	Range	Mean	Range
Autumn (n = 7)	−2.9^{ab}	−3.9 to −1.9	+74.9^{a}	+63.8 to +77.9
Winter (n = 8)	−4.2^{a}	−5.9 to −1.0	+76.5^{a}	+66.2 to +81.1
Spring (n = 8)	+0.3^{b}	−2.8 to +3.6	+70.4^{ab}	+50.6 to +78.2
Summer (n = 11)	−2.3^{b}	−5.0 to +0.1	+63.0^{b}	+52.5 to +71.7

Within a column, means followed by different letters are significantly different at α = 0.05.

year (See in the Supplementary Material). Seasonal variations of δ^{15}N-NO_3^- isotopes were used to reflect the changes of potential sources, which are mainly governed by East-Asia monsoon system. δ^{15}N-NO_3^- in precipitation varied between −5.9‰ and +3.6‰, with an annual average value of −2.4‰ (Table 6). In the winter, δ^{15}N-NO_3^- ranged from −5.9 to −1.0‰. The δ^{15}N values of coals in China varies between −6 and +4‰ with an average value of −1.5‰ (Xiao and Liu, 2011). As described in Fig. 1, the Pinghai coal-fired power plant is running in the east Daya Bay with continuous NO_x emissions throughout the year.

A positive correlation has been found between NO_3^- and $_{nss}SO_4^{2-}$ in the precipitation ($r^2 = 0.54$, $p < 0.01$, Fig. 5e), suggesting that the sources of NO_3^- might be associated with SO_4^{2-} dominated by coal combustion in the southeast China. It is reported that the main sources of NO_x emission are relevant to fossil fuel combustion in China (Liu et al., 2011, 2017). Furthermore, the $_{nss}SO_4^{2-}/SO_4^{2-}$ (51%, Fig. 5g) in winter showed fossil fuel was a significant contributor to nitrogen in precipitation. Nitrogen deposition in Daya Bay in this season could be presumed predominantly driven by the anthropogenic sources from mainland China and northern Daya Bay according to the backward trajectories (Fig. 4). A similar result was also reported in the nitrogen-polluted city in southern China (Fang et al., 2011) and the northern SCS (Yang et al., 2014). Nitrate in the precipitation had low δ^{15}N-NO_3^- value (−7.5 to −3.1‰) in southeastern China coastal area, which was in the upwind direction of Daya Bay in winter and mostly from vehicle exhausts (Chen et al., 2011; Felix and Elliott, 2014). It is reported that up to 41% of NO_x emission were from mobile sources in the region (Zheng et al., 2009). δ^{15}N-NO_3^- value in spring and was statistically different with that in winter (Table 6). As atmospheric inputs are important allochthonous sources of nitrogen, the southwest monsoon in spring may bring continental nitrogen from PRD and southeast Asia, while from mainland China by the northeast monsoon in winter (Fig. 4). $_{nss}Ca^{2+}$

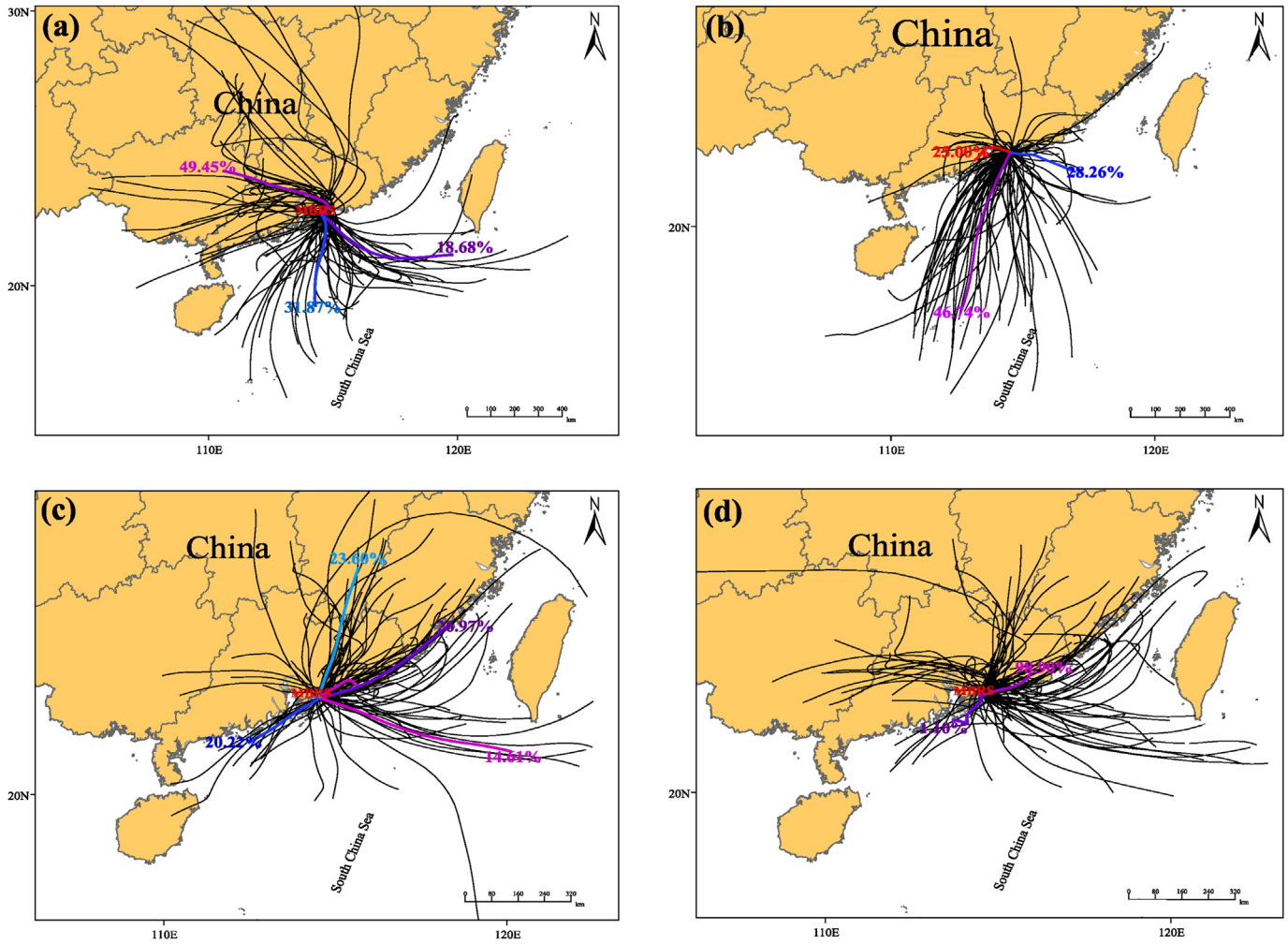

Fig. 4. Air mass transportation pathway at 500 m in four seasons, (a) spring, (b) summer, (c) autumn, and (d) winter, in Daya Bay: using HYSPLIT backward trajectory model by ARL, NOAA. (http://ready.arl.noaa.gov/HYSPLIT_traj.php).

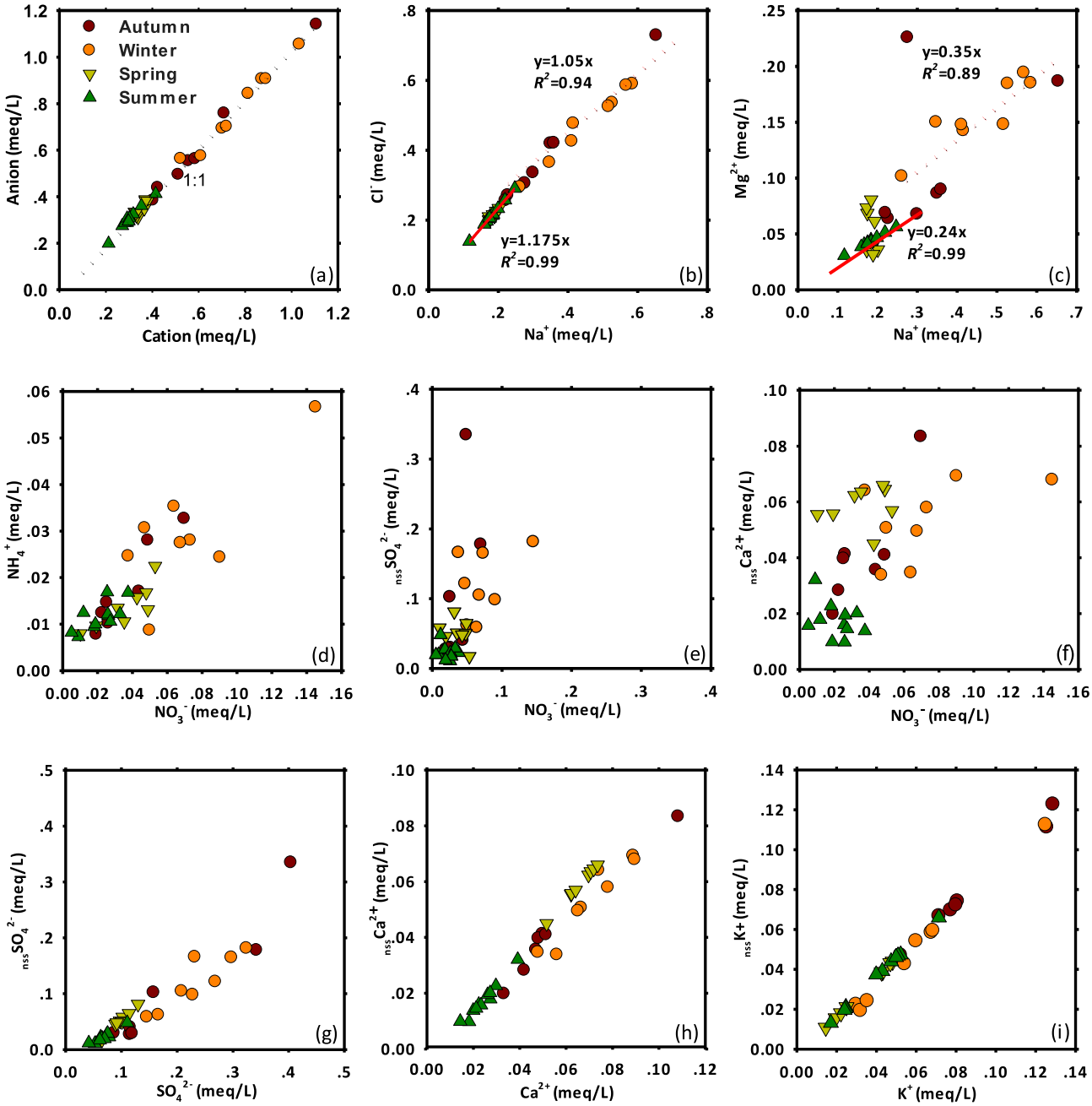

Fig. 5. Relationships for concentrations of **(a)** the total anions versus total cations, **(b)** Cl^- versus Na^+, **(c)** Mg^{2+} versus Na^+, **(d)** NH_4^+ versus NO_3^-, **(e)** $_{nss}SO_4^{2-}$ versus NO_3^-, **(f)** $_{nss}Ca^{2+}$ versus NO_3^-, **(g)** $_{nss}SO_4^{2-}$ versus SO_4^{2-}, **(h)** $_{nss}Ca^{2+}$ versus Ca^{2+}, **(i)** $_{nss}K^+$ versus K^+, in precipitation during autumn 2015 to summer 2016 one-year period. In **(b)** and **(c)**, the red dotted line represents the relationship of the two ions in winter, and the solid red line represents summer. (For interpretation of the references to colour in this figure legend, the reader is referred to the Web version of this article.)

was in high concentration and accounted a larger part of Ca^{2+} in spring and winter. Moreover, the intimate correlation between $_{nss}Ca^{2+}$ and NO_3^- (Fig. 5f, $R^2 = 0.59$, $p < 0.01$) and the ratio of $_{nss}Ca^{2+}/Ca^{2+}$ (Fig. 5h) could presumably indicate that crustal dust may be an active carrier of NO_3^- in winter. This was also reported by Hsu et al. (2014) and Streets et al. (2003) that the SCS receives Asian dust and pollution outflows and Southeast Asian biomass burning, which also may contribute to the nitrate in precipitation in Daya Bay. Based on the discussion above, we concluded that a mixture of dust and fossil fuel combustion (mainly of coal combustion and vehicle exhaust) were the predominant sources in spring and winter.

In summer, 75% air mass originated from SCS (Fig. 4) and five typhoons passed or influenced Daya Bay, which may bring large precipitation from the SCS and western Pacific (Potty et al., 2012). Air mass trajectories have shown that maritime sources could be the main pathway contributing to Daya Bay. And the Cl^-/Na^+ (1.175, Fig. 5b) and Na^+/Mg^{2+} (0.24, Fig. 5c) ratio indicated that marine input from SCS to be a potential source in this season (Xiao et al., 2017). Moreover,

$_{nss}SO_4^{2-}/SO_4^{2-}$ (Fig. 5g) showed a relatively lower ratio (31%) and $NO_3^-/_{nss}SO_4^{2-}$ ratio in summer (1.14, Fig. 5e) was higher than that in other seasons (0.90, 0.61, and 0.67 for spring, autumn and winter, respectively), indicating that nitrogen in precipitation was in a small portion from fossil fuel combustion. However, 73% of all the $\delta^{15}N$ values in summer ranged from −5.0 to +0.1‰ (average −2.3‰), which were within the range of $\delta^{15}N$-NO_x originated from vehicle exhausts (Fibiger and Hastings, 2016; Walters et al., 2015), suggesting that fossil fuel could be a considerable source in summer. Considering the northern SCS is one of the busiest shipping area consuming a large amount of fossil fuel, a mix of marine and fossil fuel sources may contribute to NO_3^- in summer. In addition, 27% of the total samples were located in the range of $\delta^{15}N$ value from lightning source NO_x (Hoering, 1957). Daya Bay is located in a subtropical area, where lightning occurs intensively in summer. According to the lightning observation in Hong Kong, west of Daya Bay, lightning occurred 33,138 times in summer, accounting for 81% of the total lightning frequency during our sampling period (http://www.weather.gov.hk/contente.htm), indicating that the contribution of lightning NO_x might increase in summer. Also, it is reported that natural NO_x emissions (soil emission) accounted for 23% of the total Asian NO_x emissions in summer, 8% in winter, and 16% annually (Zhao et al., 2015). In Eastern China, nearly 30% of NO_x was from natural sources combining lightning and biogenic emission in rainy months (Lin, 2012). However, no obvious isotopic signature of biogenic emission NO_x (soil emission) was found in this paper.

3.6. Formation process of nitrate

Seasonal variation of $\delta^{18}O$-NO_3^- was shown in Table 6. 94% of $\delta^{18}O$-NO_3^- values in this paper were within the range of +55 to +102‰, suggesting that the main $\delta^{18}O$-NO_3^- formation process may derive from OH radical and N_2O_5 pathway (stated in the introduction) (Hastings et al., 2003; Johnston and Thiemens, 1997; Xiao et al., 2015). The highest mean value of $\delta^{18}O$-NO_3^- (+76.5‰) occurred in winter, while the lowest mean value (+63.0‰) was in summer. There was a significant difference between winter and summer, which implies distinct $\delta^{18}O$-NO_3^- formation processes in these two seasons.

In winter, strong northeast winds prevail in Daya Bay (Fig. 4b) (Hsu et al., 2014). NO_x from mainland China and northern Daya Bay significantly contribute to nitrogen deposition in precipitation. NO_x with low $\delta^{15}N$-NO_3^- value originated from fossil fuel combustion originating from Chinese mainland cities, and more O_3 contributed to NO_3 due to the heavy pollution (4 and 5). In spring, the $\delta^{15}N$-NO_3^- value was significantly different with that in winter, while no difference was found of $\delta^{18}O$-NO_3^-. This implies that there are distinct sources of nitrogen but analogous formation pathways of nitrate in spring and winter, most probably due to the contribution of air pollutants in the nitrate formation process (Chen et al., 2010; Zheng et al., 2012). In spring and winter, the air temperature was relatively lower than summer. A negative correlation was previously found between $\delta^{18}O$-NO_3 and temperature (Fang et al., 2011). NO_2 is oxidized by O_3 to produce NO_3 radical (NO_3) (5), which subsequently combines with NO_2 to form dinitrogen pentoxide (N_2O_5) (6). The hydrolysis of N_2O_5 yields HNO_3 (7). This pathway is most prevalent during winter as N_2O_5 is thermally unstable (Fang et al., 2011). In addition, pollutants like dimethylsulfide (DMS) or hydrocarbons (HC) were involved with O_3 during the formation of NO_3^- by a DMS/HC pathway (8) (Alexander et al., 2009). Furthermore, halogens, such as chlorine oxide (ClO), were at high levels due to heavy pollution (Ji et al., 2013), NO or NO_2 would form to NO_3 by combining with ClO (10) (Altieri et al., 2013; Gobel et al., 2013). Halogen oxides' involvement made the $\delta^{18}O$-NO_3 value higher because O_3 contributes to ClO formation (9-11) (Alexander et al., 2009; Altieri et al., 2013; Fang et al., 2011). Although O atom by DMS/HC and Halogen oxides pathway have higher abundance, it could be diluted by other pathways (OH or N_2O_5 pathways) due to their lower proportion in the formation of NO_3^-. (4-11) simply described the producing of HNO_3 involving with O_3, though the chemical process was more complicated. Therefore, in winter, N_2O_5 was the predominant pathway that controls the formation of nitrate, while DMS/HC and halogens could be additional pathways that make the $\delta^{18}O$-NO_3^- value higher than that in summer.

$$NO + O_3 \rightarrow NO_2 + O_2 \quad (4)$$

$$NO_2 + O_3 \rightarrow NO_3 + O_2 \quad (5)$$

$$NO_2 + NO_3 \leftrightarrow N_2O_5 \quad (6)$$

$$N_2O_5 + H_2O \rightarrow HNO_3 \quad (7)$$

$$NO_3 + DMS/HC \rightarrow HNO_3 \quad (8)$$

$$Cl/Br + O_3 \rightarrow ClO/BrO + O_2 \quad (9)$$

$$NO_2 + ClO \rightarrow ClONO_2 \quad (10)$$

$$ClONO_2 + NaCl \rightarrow NaNO_3 + Cl_2 \quad (11)$$

Higher $\delta^{15}N$-NO_3^- and lower $\delta^{18}O$-NO_3^- in summer are found compared with winter. Values of $\delta^{15}N$-NO_3^- and $\delta^{18}O$-NO_3^- were statistically different to winter (Table 6), implying a different formation process of nitrate. Typhoons prevail in the SCS in summer, and air mass back-trajectory evidence showed that 75% of the air mass was from the SCS, suggesting that $\delta^{15}N$-NO_3^- increased and $\delta^{18}O$-NO_3 decreased during transport from remote seas to the coastal area. The high $\delta^{15}N$-NO_3 value was associated with low $\delta^{18}O$-NO_3 at Daya Bay in summer. It should be noted that O_3 concentration is relatively lower in summer ($0.62\,\mu g\,m^{-3}$, $1.22\,\mu g\,m^{-3}$ in spring $1.62\,\mu g\,m^{-3}$ in autumn, $1.19\,\mu g\,m^{-3}$ in winter) along the PRD (Lee et al., 2014), and OH concentrations are in high level (OH is photolytically produced, (12)) (Alexander et al., 2009). Photochemistry is the main driver for chemical activity in the atmosphere in summer (Aneja et al., 2001), as the radiation was strong in Daya Bay, which may induce more OH radicals (12). The hydrolysis of NO_2 yields HONO and HNO_3 (13). And HONO was photolysis to OH (14). It is likely that an OH radical pathway was most probably dominant in the formation of nitrate in summer. OH radical pathways are also found in Guangzhou (Fang et al., 2011) and the SCS (Xiao et al., 2015; Yang et al., 2014) in rainy months. A negative relationship was found between $\delta^{15}N$-NO_3^- and $\delta^{18}O$-NO_3^- ($R^2 = 0.64$, $p = 0.0058$) in summer (Fig. 6). Similar results were found in the marine environment (Altieri et al., 2013; Gobel et al., 2013; Yang et al., 2014), which implies that nitrate formation was regulated by OH radicals from maritime sources in summer.

$$NO_2 + OH \rightarrow HNO_3 \quad (12)$$

$$2NO_2 + H_2O \leftrightarrow HONO + HNO_3 \quad (13)$$

$$HONO + hv \rightarrow NO + OH \quad (14)$$

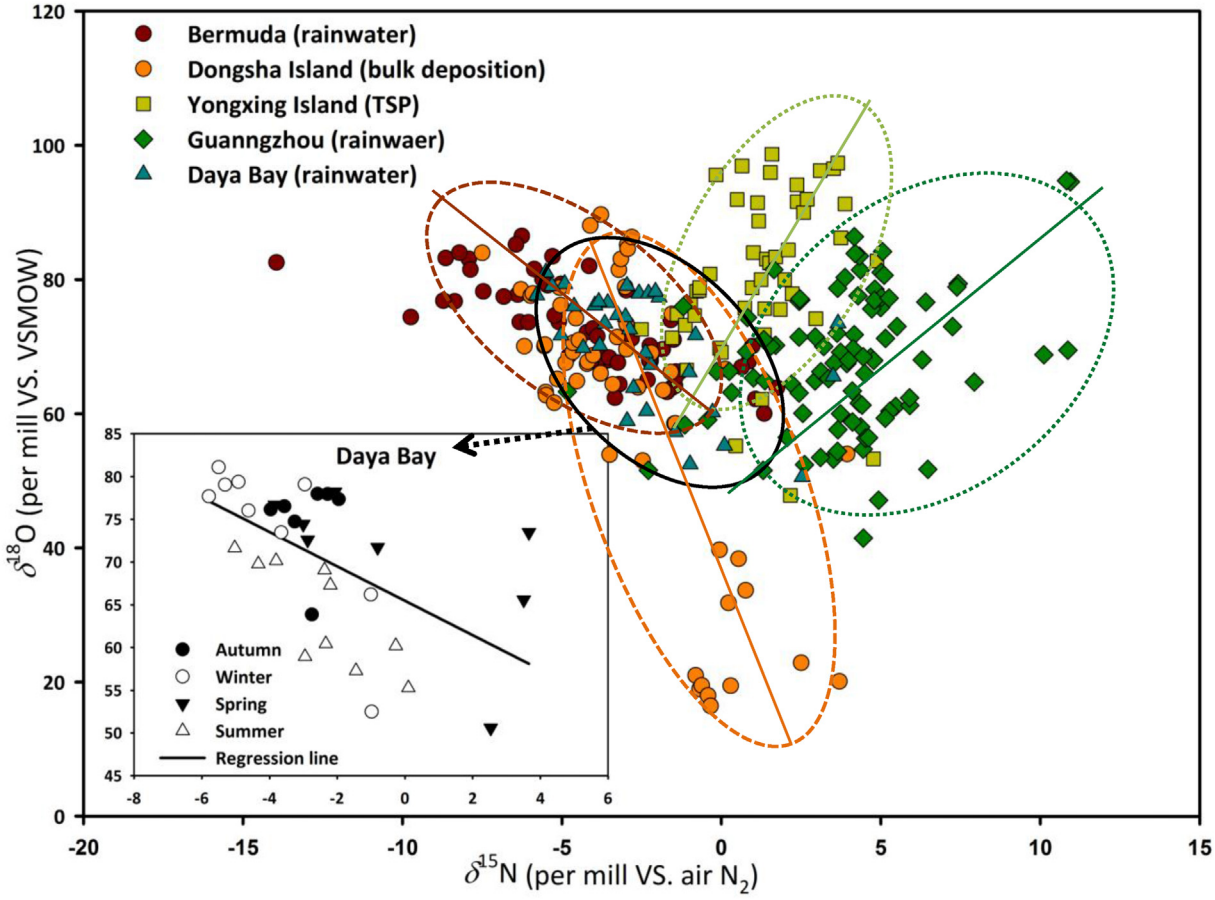

Fig. 6. The relationship between δ^{15}N-NO_3^- and δ^{18}O-NO_3^- in rainwater at Bermuda (Altieri et al., 2013), in bulk deposition at Dongsha Island (Yang et al., 2014), in TSP at Yongxiang Island (Xiao et al., 2015), in rainwater at Guangzhou (Fang et al., 2011), and in rainwater at Daya Bay (**black circle**). Correlation between δ^{15}N-NO_3^- and δ^{18}O-NO_3^- values in precipitation (n = 34). The solid line indicates the regression line for the entire data set of Daya Bay.

4. Conclusions

The atmospheric deposition fluxes of TDN in precipitation was 132.5 mmol m^{-2}·yr^{-1} from October 2015 to September 2016, which accounted for 37.8% of the total input of nitrogen into Daya Bay. DIN accounted for 62.6% of the TDN, and NO_3^- accounted for 77.8% of the DIN. DON acted as a significant contributor to nitrogen in precipitation. Further study on the compositions and specific sources of DON should be clarified in the future due to the important role of DON. The TDN flux was higher in spring and summer, and lower in winter months. The wet N deposition flux accounted for 37.8% of the total nitrogen input. In winter, fossol fuel (coal combustion and vehicle exhausts) and dust from mainland China transported by northeast monsoon are the main sources of nitrogen, while fossil fuel (coal and vehicle exhausts) and dust from PRD and southeast Asia delivered by southwest monsoon were proved to be the probable sources in spring. A mixture of marine, vehicle exhaust and lightning were the main sources of nitrogen in summer. Atmospheric nitrogen deposition in precipitation was strongly regulated by the East Asia Monsoon system in spring and winter (southwest monsoon and northeast monsoon, respectively) and affected by the typhoons in summer. OH pathway was dominant in the chemical formation process of nitrate in summer, while N_2O_5 + DMS/HC pathways in winter and spring. Therefore, it is necessary to control the emission in the upwind direction in governing the atmospheric nitrogen inputs to Daya Bay.

Acknowledgements

This work was supported by the National Program on Key Basic Research Project of China (No.2015CB452901, No.2015CB452905), and National Natural Science Foundation of China (NSFC, No.41406128 and No. 41730529). Peter Macreadie's involvement was supported by an Australian Research Council Linkage Project (LP160100242). The MBRS was thanked for sampling supporting. We also gratefully acknowledge the NOAA Air Resources Laboratory (ARL) for the provision of the HYSPLIT transport and dispersion model and READY website (http://www.ready.noaa.gov). Hong Kong Observatory was also thanked for supporting lightning data.

Appendix A. Supplementary data

Supplementary data related to this article can be found at doi:http://dx.doi.org/10.1016/j.atmosenv.2018.03.037.

References

Alexander, B., Hastings, M.G., Allman, D.J., Dachs, J., Thornton, J.A., Kunasek, S.A., 2009. Quantifying atmospheric nitrate formation pathways based on a global model of the oxygen isotopic composition (delta O-17) of atmospheric nitrate. Atmos. Chem. Phys. 9, 5043–5056.

Altieri, K.E., Hastings, M.G., Gobel, A.R., Peters, A.J., Sigman, D.M., 2013. Isotopic composition of rainwater nitrate at Bermuda: the influence of air mass source and chemistry in the marine boundary layer. J. Geophys. Res. Atmos. 118, 11304–11316.

Altieri, K.E., Hastings, M.G., Peters, A.J., Oleynik, S., Sigman, D.M., 2014. Isotopic evidence for a marine ammonium source in rainwater at Bermuda. Global Biogeochem. Cycles 28, 1066–1080.

Aneja, V.P., Roelle, P.A., Murray, G.C., Southerland, J., Erisman, J.W., Fowler, D., Asman, W.A.H., Patni, N., 2001. Atmospheric nitrogen compounds II: emissions, transport, transformation, deposition and assessment. Atmos. Environ. 35, 1903–1911.

Bencs, L., Krata, A., Horemans, B., Buczynska, A.J., Dirtu, A.C., Godoi, A.F.L., Godoi, R.H.M., Potgieter-Vermaak, S., Van Grieken, R., 2009. Atmospheric nitrogen fluxes at the Belgian coast: 2004-2006. Atmos. Environ. 43, 3786–3798.

Calderon, S.M., Poor, N.D., Campbell, S.W., 2007. Estimation of the particle and gas scavenging contributions to wet deposition of organic nitrogen. Atmos. Environ. 41, 4281–4290.
Chen, J., Lu, P., Chen, Z.Y., Yan, H.H., Li, L.S., 2014. Atmospheric deposition of nitrogen and phosphorus at Daya Bay in Huizhou during spring and summer. J. Trop. Oceanol. 33, 109–114 (in Chinese with English abstract).
Chen, N.W., Hong, H.S., Huang, Q.J., Wu, J.Z., 2011. Atmospheric nitrogen deposition and its long-term dynamics in a southeast China coastal area. J. Environ. Manag. 92, 1663–1667.
Chen, Y.X., Chen, H.Y., Wang, W., Yeh, J.X., Chou, W.C., Gong, G.C., Tsai, F.J., Huang, S.J., Lin, C.T., 2015. Dissolved organic nitrogen in wet deposition in a coastal city (Keelung) of the southern East China Sea: origin, molecular composition and flux. Atmos. Environ. 112, 20–31.
Chen, Z.Y., Li, K.M., Lin, W.S., Liu, A.P., 2010. Atmospheric dry and wet deposition of nitrogen and phosphorus in the Pearl River Estuary. Environ. Pollut. Contr. 32, 53–57 (in Chinese with English abstract).
Cornell, S.E., 2011. Atmospheric nitrogen deposition: revisiting the question of the importance of the organic component. Environ. Pollut. 159, 2214–2222.
Duce, R.A., LaRoche, J., Altieri, K., Arrigo, K.R., Baker, A.R., Capone, D.G., Cornell, S., Dentener, F., Galloway, J., Ganeshram, R.S., Geider, R.J., Jickells, T., Kuypers, M.M., Langlois, R., Liss, P.S., Liu, S.M., Middelburg, J.J., Moore, C.M., Nickovic, S., Oschlies, A., Pedersen, T., Prospero, J., Schlitzer, R., Seitzinger, S., Sorensen, L.L., Uematsu, M., Ulloa, O., Voss, M., Ward, B., Zamora, L., 2008. Impacts of atmospheric anthropogenic nitrogen on the open ocean. Science 320, 893–897.
Duce, R.A., Liss, P.S., Merrill, J.T., Atlas, E.L., Buat-Menard, P., Hicks, B.B., Miller, J.M., Prospero, J.M., Arimoto, R., Church, T.M., Ellis, W., Galloway, J.N., Hansen, L., Jickells, T.D., Knap, A.H., Reinhardt, K.H., Schneider, B., Soudine, A., Tokos, J.J., Tsunogai, S., Wollast, R., Zhou, M., 1991. The atmospheric input of trace species to the world ocean. Global Biogeochem. Cycles 5, 193–259.
Fang, Y.T., Koba, K., Wang, X.M., Wen, D.Z., Li, J., Takebayashi, Y., Liu, X.Y., Yoh, M., 2011. Anthropogenic imprints on nitrogen and oxygen isotopic composition of precipitation nitrate in a nitrogen-polluted city in southern China. Atmos. Chem. Phys. 11, 1313–1325.
Felix, J.D., Elliott, E.M., 2014. Isotopic composition of passively collected nitrogen dioxide emissions: vehicle, soil and livestock source signatures. Atmos. Environ. 92, 359–366.
Felix, J.D., Elliott, E.M., Shaw, S.L., 2012. Nitrogen isotopic composition of coal-fired power plant NOx: influence of emission controls and implications for global emission inventories. Environ. Sci. Technol. 46, 3528–3535.
Fibiger, D.L., Hastings, M.G., 2016. First measurements of the nitrogen isotopic composition of NOx from biomass burning. Environ. Sci. Technol. 50, 11569–11574.
Galloway, J.N., Aber, J.D., Erisman, J.W., Seitzinger, S.P., Howarth, R.W., Cowling, E.B., Cosby, B.J., 2003. The nitrogen cascade. Bioscience 53, 341–356.
Galloway, J.N., Townsend, A.R., Erisman, J.W., Bekunda, M., Cai, Z.C., Freney, J.R., Martinelli, L.A., Seitzinger, S.P., Sutton, M.A., 2008. Transformation of the nitrogen cycle: recent trends, questions, and potential solutions. Science 320, 889–892.
Gao, Y., Kennish, M.J., Flynn, A.M., 2007. Atmospheric nitrogen deposition to the New Jersey coastal waters and its implications. Ecol. Appl. 17, S31–S41.
Gioda, A., Reyes-Rodriguez, G.J., Santos-Figueroa, G., Collett, J.L., Decesari, S., Ramos, M.D.K.V., Netto, H.J.C.B., Neto, F.R.D., Mayol-Bracero, O.L., 2011. Speciation of water-soluble inorganic, organic, and total nitrogen in a background marine environment: cloud water, rainwater, and aerosol particles. J. Geophys. Res. Atmos. 116.
Gobel, A.R., Altieri, K.E., Peters, A.J., Hastings, M.G., Sigman, D.M., 2013. Insights into anthropogenic nitrogen deposition to the North Atlantic investigated using the isotopic composition of aerosol and rainwater nitrate. Geophys. Res. Lett. 40, 5977–5982.
Hastings, M.G., Sigman, D.M., Lipschultz, F., 2003. Isotopic evidence for source changes of nitrate in rain at Bermuda. J. Geophys. Res. Atmos. 108.
Heaton, T.H.E., 1990. $^{15}N/^{14}N$ ratios of NO_x from vehicle engines and coal-fired power stations. Tellus 42B, 304–307.
Hoering, T., 1957. The isotopic composition of the ammonia and the nitrate Ion in rain. Geochem. Cosmochim. Acta 12, 97–102.
Hsu, S.C., Gong, G.C., Shiah, F.K., Hung, C.C., Kao, S.J., Zhang, R., Chen, W.N., Chen, C.C., Chou, C.C.K., Lin, Y.C., 2014. Sources, solubility, and acid processing of aerosol iron and phosphorous over the South China Sea: east Asian dust and pollution outflows vs. Southeast Asian biomass burning. Atmos. Chem. Phys. 14, 21433–21472.
Huang, Q., Guan, Y.P., 2012. Does the Asian monsoon modulate tropical cyclone activity over the South China Sea? Chin. J. Oceanol. Limnol. 30, 960–965.
Huang, X.F., Li, X.A., He, L.Y., Feng, N., Hu, M., Niu, Y.W., Zeng, L.W., 2010. 5-Year study of rainwater chemistry in a coastal mega-city in South China. Atmos. Res. 97, 185–193.
Huang, Z.J., Wang, S.S., Zheng, J.Y., Yuan, Z.B., Ye, S.Q., Kang, D.W., 2015. Modeling inorganic nitrogen deposition in Guangdong province, China. Atmos. Environ. 109, 147–160.
Ji, Y.M., Wang, H.H., Gao, Y.P., Li, G.Y., An, T.C., 2013. A theoretical model on the formation mechanism and kinetics of highly toxic air pollutants from halogenated formaldehydes reacted with halogen atoms. Atmos. Chem. Phys. 13, 11277–11286.
Jia, G.D., Chen, F.J., 2010. Monthly variations in nitrogen isotopes of ammonium and nitrate in wet deposition at Guangzhou, south China. Atmos. Environ. 44, 2309–2315.
Johnston, J.C., Thiemens, M.H., 1997. The isotopic composition of tropospheric ozone in three environments. J. Geophys. Res. Atmos. 102, 25395–25404.
Karthikeyan, S., He, J., Palani, S., Balasubramanian, R., Burger, D., 2009. Determination of total nitrogen in atmospheric wet and dry deposition samples. Talanta 77, 979–984.
Keene, W.C., Montag, J.A., Maben, J.R., Southwell, M., Leonard, J., Church, T.M., Moody, J.L., Galloway, J.N., 2002. Organic nitrogen in precipitation over eastern north America. Atmos. Environ. 36, 4529–4540.
Kim, T.W., Lee, K., Duce, R., Liss, P., 2014. Impact of atmospheric nitrogen deposition on phytoplankton productivity in the South China Sea. Geophys. Res. Lett. 41, 3156–3162.
Kocak, M., Kubilay, N., Tugrul, S., Mihalopoulos, N., 2010. Atmospheric nutrient inputs to the northern levantine basin from a long-term observation: sources and comparison with riverine inputs. Biogeosciences 7, 4037–4050.
Laouali, D., Galy-Lacaux, C., Diop, B., Delon, C., Orange, D., Lacaux, J.P., Akpo, A., Lavenu, F., Gardrat, E., Castera, P., 2012. Long term monitoring of the chemical composition of precipitation and wet deposition fluxes over three Sahelian savannas. Atmos. Environ. 50, 314–327.
Lee, Y.C., Shindell, D.T., Faluvegi, G., Wenig, M., Lam, Y.F., Ning, Z., Hao, S., Lai, C.S., 2014. Increase of ozone concentrations, its temperature sensitivity and the precursor factor in South China. Tellus B 66.
Li, D., Wang, X., 2008. Nitrogen isotopic signature of soil-released nitric oxide (NO) after fertilizer application. Atmos. Environ. 42, 4747–4754.
Lin, J.T., 2012. Satellite constraint for emissions of nitrogen oxides from anthropogenic, lightning and soil sources over East China on a high-resolution grid. Atmos. Chem. Phys. 12, 2881–2898.
Liu, L., Zhang, X.Y., Wang, S.Q., Lu, X.H., Ouyang, X.Y., 2016. A review of spatial variation of inorganic nitrogen (N) wet deposition in China. Plos One 11.
Liu, X., Xu, W., Duan, L., Du, E., Pan, Y., Lu, X., Zhang, L., Wu, Z., Wang, X., Zhang, Y., Shen, J., Song, L., Feng, Z., Liu, X., Song, W., Tang, A., Zhang, Y., Zhang, X., Collett, J.L., 2017. Atmospheric nitrogen emission, deposition, and air quality impacts in China: an overview. Curr. Pollut. Rep. 1–13.
Liu, X.J., Duan, L., Mo, J.M., Du, E.Z., Shen, J.L., Lu, X.K., Zhang, Y., Zhou, X.B., He, C.N., Zhang, F.S., 2011. Nitrogen deposition and its ecological impact in China: an overview. Environ. Pollut. 159, 2251–2264.
Liu, X.J., Zhang, Y., Han, W.X., Tang, A.H., Shen, J.L., Cui, Z.L., Vitousek, P., Erisman, J.W., Goulding, K., Christie, P., Fangmeier, A., Zhang, F.S., 2013. Enhanced nitrogen deposition over China. Nature 494, 459–462.
Luo, X.S., Tang, A.H., Shi, K., Wu, L.H., Li, W.Q., Shi, W.Q., Shi, X.K., Erisman, J.W., Zhang, F.S., Liu, X.J., 2014. Chinese coastal seas are facing heavy atmospheric nitrogen deposition. Environ. Res. Lett. 9.
Meng, Z.Y., Zhang, R.J., Lin, W.L., Jia, X.F., Yu, X.M., Yu, X.L., Wang, G.H., 2014. Seasonal variation of ammonia and ammonium aerosol at a background station in the Yangtze River Delta region, China. Aerosol. Air Qual. Res. 14, 756–766.
Michalski, G., Kolanowski, M., Riha, K.M., 2015. Oxygen and nitrogen isotopic composition of nitrate in commercial fertilizers, nitric acid, and reagent salts. Isot. Environ. Health Stud. 51, 382–391.
Morin, S., Savarino, J., Frey, M.M., Domine, F., Jacobi, H.W., Kaleschke, L., Martins, J.M.F., 2009. Comprehensive isotopic composition of atmospheric nitrate in the Atlantic Ocean boundary layer from 65 degrees S to 79 degrees N. J. Geophys. Res. Atmos. 114.
Owens, N.J.P., Galloway, J.N., Duce, R.A., 1992. Episodic atmospheric nitrogen deposition to oligotrophic oceans. Nature 357, 397–399.
Paerl, H.W., Dennis, R.L., Whitall, D.R., 2002. Atmospheric deposition of nitrogen: implications for nutrient over-enrichment of coastal waters. Estuaries 25, 677–693.
Potty, J., Oo, S.M., Raju, P.V.S., Mohanty, U.C., 2012. Performance of nested WRF model in typhoon simulations over West Pacific and South China Sea. Nat. Hazards 63, 1451–1470.
Qi, J.H., Shi, J.H., Gao, H.W., Sun, Z., 2013. Atmospheric dry and wet deposition of nitrogen species and its implication for primary productivity in coastal region of the Yellow Sea, China. Atmos. Environ. 81, 600–608.
Ren, X.W., Jiang, G.Q., Liu, A.P., Li, K.M., 2013. Study on the estimation of the pollutant input flux from the main rivers to Daya Bay. In: Annual Meeting of the Chinese Academy of Environmental Sciences (2013), Kunming, pp. 2912–2921 (In Chinese).
Rolph, G., Stein, A., Stunder, B., 2017. Real-time Environmental applications and display sYstem: ready. Environ. Model. Software 95, 210–228.
Sigman, D.M., Casciotti, K.L., Andreani, M., Barford, C., Galanter, M., Bohlke, J.K., 2001. A bacterial method for the nitrogen isotopic analysis of nitrate in seawater and freshwater. Anal. Chem. 73, 4145–4153.
Spokes, L.J., Jickells, T.D., 2005. Is the atmosphere really an important source of reactive nitrogen to coastal waters? Continent. Shelf Res. 25, 2022–2035.
Stein, A.F., Draxler, R.R., Rolph, G.D., Stunder, B.J.B., Cohen, M.D., Ngan, F., 2015. Noaa's Hysplit atmospheric transport and dispersion modeling system. Bull. Am. Meteorol. Soc. 96, 2059–2077.
Streets, D.G., Yarber, K.F., Woo, J.H., Carmichael, G.R., 2003. Biomass burning in Asia: annual and seasonal estimates and atmospheric emissions. Global Biogeochem. Cycles 17.
Valigura, R.A., Alexander, R.B., Castro, M.S., Meyers, T.P., Paerl, H.W., Stacey, P.E., Turner, R.E., 2001. Nitrogen Loading in Coastal Water Bodies: an Atmospheric Perspective.
Violaki, K., Zarbas, P., Mihalopoulos, N., 2010. Long-term measurements of dissolved organic nitrogen (DON) in atmospheric deposition in the Eastern Mediterranean: fluxes, origin and biogeochemical implications. Mar. Chem. 120, 179–186.
Walters, W.W., Goodwin, S.R., Michalski, G., 2015. Nitrogen stable isotope composition (delta N-15) of vehicle-emitted NOx. Environ. Sci. Technol. 49, 2278–2285.
Wang, Y.S., Lou, Z.P., Sun, C.C., Sun, S., 2008. Ecological environment changes in Daya bay, China, from 1982 to 2004. Mar. Pollut. Bull. 56, 1871–1879.
Widory, D., 2007. Nitrogen isotopes: tracers of origin and processes affecting PM10 in the atmosphere of Paris. Atmos. Environ. 41, 2382–2390.
Wu, M.L., Wang, Y.S., Wang, Y.T., Yin, J.P., Dong, J.D., Jiang, Z.Y., Sun, F.L., 2017. Scenarios of nutrient alterations and responses of phytoplankton in a changing Daya Bay, South China Sea. J. Mar. Syst. 165, 1–12.
Wu, Y., Zhang, J., Liu, S., Jiang, Z., Huang, X., 2018. Aerosol concentrations and atmospheric dry deposition fluxes of nutrients over Daya Bay, South China Sea. Mar. Pollut. Bull. 128, 106–114.
Xiao, H.W., Xiao, H.Y., Luo, L., Shen, C.Y., Long, A.M., Chen, L., Long, Z.H., Li, D.N., 2017. Atmospheric aerosol compositions over the South China Sea: temporal variability and source apportionment. Atmos. Chem. Phys. 17, 3199–3214.
Xiao, H.W., Xie, L.H., Long, A.M., Ye, F., Pan, Y.P., Li, D.N., Long, Z.H., Chen, L., Xiao,

H.Y., Liu, C.Q., 2015. Use of isotopic compositions of nitrate in TSP to identify sources and chemistry in South China Sea. Atmos. Environ. 109, 70–78.
Xiao, H.Y., Liu, C.Q., 2011. The elemental and isotopic composition of sulfur and nitrogen in Chinese coals. Org. Geochem. 42, 84–93.
Xing, J.W., Song, J.M., Yuan, H.M., Li, X.G., Li, N., Duan, L.Q., Kang, X.M., Wang, Q.D., 2017. Fluxes, seasonal patterns and sources of various nutrient species (nitrogen, phosphorus and silicon) in atmospheric wet deposition and their ecological effects on Jiaozhou Bay, North China. Sci. Total Environ. 576, 617–627.
Xu, W., Luo, X.S., Pan, Y.P., Zhang, L., Tang, A.H., Shen, J.L., Zhang, Y., Li, K.H., Wu, Q.H., Yang, D.W., Zhang, Y.Y., Xue, J., Li, W.Q., Li, Q.Q., Tang, L., Lu, S.H., Liang, T., Tong, Y.A., Liu, P., Zhang, Q., Xiong, Z.Q., Shi, X.J., Wu, L.H., Shi, W.Q., Tian, K., Zhong, X.H., Shi, K., Tang, Q.Y., Zhang, L.J., Huang, J.L., He, C.E., Kuang, F.H., Zhu, B., Liu, H., Jin, X., Xin, Y.J., Shi, X.K., Du, E.Z., Dore, A.J., Tang, S., Collett, J.L., Goulding, K., Sun, Y.X., Ren, J., Zhang, F.S., Liu, X.J., 2015. Quantifying atmospheric nitrogen deposition through a nationwide monitoring network across China. Atmos. Chem. Phys. 15, 12345–12360.
Xu, Z.H., Guo, Z.R., Xu, X., Huang, D.J., Sun, X.X., Jiang, L.M., Yang, J.F., 2014. The impact of nutrient enrichment on the phytoplankton and bacterioplankton community during a mesocosm experiment in Nan'ao of Daya Bay. Mar. Biol. Res. 10, 374–382.
Yang, J.Y.T., Hsu, S.C., Dai, M.H., Hsiao, S.S.Y., Kao, S.J., 2014. Isotopic composition of water-soluble nitrate in bulk atmospheric deposition at Dongsha Island: sources and implications of external N supply to the northern South China Sea. Biogeosciences 11, 1833–1846.
Yu, J., Tang, D.L., Imsang, O., Yao, L.J., 2007. Response of harmful algal blooms to environmental changes in Daya Bay, China. Terr. Atmos. Ocean Sci. 18, 1011–1027.
Zamora, L.M., Prospero, J.M., Hansell, D.A., 2011. Organic nitrogen in aerosols and precipitation at Barbados and Miami: implications regarding sources, transport and deposition to the western subtropical North Atlantic. J. Geophys. Res. Atmos. 116.
Zhang, L.M., Gong, S.L., Padro, J., Barrie, L., 2001. A size-segregated particle dry deposition scheme for an atmospheric aerosol module. Atmos. Environ. 35, 549–560.
Zhang, Y., Song, L., Liu, X.J., Li, W.Q., Lu, S.H., Zheng, L.X., Bai, Z.C., Cai, G.Y., Zhang, F.S., 2012. Atmospheric organic nitrogen deposition in China. Atmos. Environ. 46, 195–204.
Zhao, Y., Zhang, L., Pan, Y., Wang, Y., Paulot, F., Henze, D.K., 2015. Atmospheric nitrogen deposition to the northwestern Pacific: seasonal variation and source attribution. Atmos. Chem. Phys. 15, 10905–10924.
Zheng, D.N., Wang, X.S., Xie, S.D., Duan, L., Chen, D.S., 2014. Simulation of atmospheric nitrogen deposition in China in 2010. China Environ. Sci. 34, 1089–1097 (in Chinese with English abstract).
Zheng, J., Zhang, L., Che, W., Zheng, Z., Yin, S., 2009. A highly resolved temporal and spatial air pollutant emission inventory for the Pearl River Delta region, China and its uncertainty assessment. Atmos. Environ. 43, 5112–5122.
Zheng, J.Y., Yin, S.S., Kang, D.W., Che, W.W., Zhong, L.J., 2012. Development and uncertainty analysis of a high-resolution NH3 emissions inventory and its implications with precipitation over the Pearl River Delta region, China. Atmos. Chem. Phys. 12, 7041–7058.
Zou, W., Wang, H.Y., Gao, J.L., 2011. Fluxes of N and P into Daya bay by atmospheric deposition. Mar. Environ. Sci. 30, 843–846 (in Chinese with English abstract).